

ENGINEERING RESEARCH INSTITUTE  
UNIVERSITY OF MICHIGAN  
ANN ARBOR

THE NEGATIVE CAPACITY AMPLIFIER

Technical Report No. 33  
Electronic Defense Group  
Department of Electrical Engineering

By: *enard*  
L. C. Beavis

Approved by:

*H. W. Welch, Jr.*  
H. W. Welch, Jr.

*L. W. Orr.*  
L. W. Orr

Project 2262

TASK ORDER NO. EDG-4  
CONTRACT NO. DA-36-039 sc-63203  
SIGNAL CORPS, DEPARTMENT OF THE ARMY  
DEPARTMENT OF ARMY PROJECT NO. 3-99-04-042  
SIGNAL CORPS PROJECT NO. 194B  
PLACED BY: SIGNAL CORPS ENGINEERING LABORATORY  
FORT MONMOUTH, NEW JERSEY

August, 1954

en sm  
UMR0288

## TABLE OF CONTENTS

	Page
LIST OF ILLUSTRATIONS	iii
ACKNOWLEDGEMENTS	iv
ABSTRACT	v
1. INTRODUCTION	1
2. CIRCUIT CONSIDERATIONS	2
3. EXPERIMENTAL RESULTS	
3.1 Actual Circuits	7
3.2 Explanation of Graphs	7
3.3 Summary of Results	13
3.4 Application to Dielectric Tuned Receivers	15
4. CONCLUSIONS	17
APPENDIX A	18
APPENDIX B	19
REFERENCES	23
DISTRIBUTION LIST	24

## LIST OF ILLUSTRATIONS

<u>Fig. No.</u>	<u>Title</u>	<u>Page</u>
1	Block Diagram of Negative Capacity Element	2
2	Thevenin Equivalent of Block Diagram of Negative Capacity Amplifier	3
3	Circuit Diagram of the Negative Capacity Element	4
4	Graph of $G_i$ Vs. Frequency with $C_k$ as a Parameter	9
5	Graph of $G_i$ Vs. Frequency with $C_n$ as a Parameter	10
6	Graph of $C_i$ Vs. Frequency with $C_n$ as a Parameter	11
7	Oscillator Circuit Used in Conjunction with the Negative Capacity Element	14
8	Tuning Curves of a Dielectric Tuned Receiver	16
9	Block Diagram of Negative Capacity Amplifier	19
10	Simplified Circuit of Negative Capacity Amplifier	21
11	Equivalent Current Generator Circuit of Figure 8	21

#### ACKNOWLEDGEMENT

The author wishes to thank Dr. L. W. Orr for his guiding influence in this investigation. The author also wishes to thank Dr. J. L. Stewart and Mr. H. Diamond for their assistance.

## ABSTRACT

The production of a negative-capacity by means of a two stage amplifier has been investigated with the hope that it would be helpful in extending the tuning range of existing ferroelectric capacitors. It is found that the negative capacity thus produced is limited in application because of its inability to handle input voltages above 3 or 4 volts rms, and to operate successfully at frequencies above 3 mc.

Although the negative-capacity circuit may be effective in reducing the capacitance of an external circuit, its practical application is restricted to external circuits having a minimum positive capacitance; the actual value of this minimum positive capacitance is dependent upon the amount of negative capacitance to be added to the external circuit.

ERRATA

TECHNICAL REPORT NO. 33

Page 5 --- Figure 3,  $C_Q$  should be  $C_k$

Page 22 --- Equation 21 should read -

$$T = C_o^n C_o^i (G_P + G^i) + C_k C_o^n G_2 + C_k C_o^i (G_3 + G_P) + G_k C_o^n C_o^i$$

Page 23 --- Reference No. 4 - (P. E. Bell) should read (P. R. Bell)

## THE NEGATIVE CAPACITY AMPLIFIER

1. INTRODUCTION

The negative capacity amplifier is an active circuit having a negative capacitance input. It was investigated for possible incorporation in an electric-tuned oscillator or rf amplifier circuit (Ref. 1) to increase the tuning range available with existing ferroelectric capacitors. These capacitors have a capacitance which varies as a function of applied dc electric field, permitting electric tuning of rf oscillators and amplifiers.

The maximum range of electric tuning is now limited by the ratio of the maximum to minimum capacitance of a particular capacitor. For instance, a ferroelectric capacitor may have an effective range of from 25 to 200  $\mu\text{mf}$  with the use of a reasonable bias field. In parallel with a fixed inductance, this will give a tuning range of about  $\sqrt{200/25}$  or 2.8. However, if some method could be found to increase this capacity ratio, the tuning range would be correspondingly increased.

Increasing the capacity ratio might be accomplished by subtracting capacity from the maximum and minimum ferroelectric values. For instance, if -20  $\mu\text{mf}$  was shunted with the 25-200  $\mu\text{mf}$  variable dielectric capacitor, the new effective capacity range would be from 5-180  $\mu\text{mf}$ , which more than doubles the original tuning range. Although these hypothetical conditions were not duplicated, the tuning range was increased from 2:1 to 2.7:1.

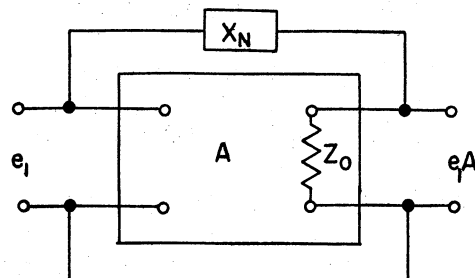
2. CIRCUIT CONSIDERATIONS

It might be well to define here exactly what a negative capacity is and how it may be produced. A negative capacity offers a reactive component to the circuit  $x_c = j/\omega C$  which differs from a positive capacitive reactance only in the sign preceeding the  $j$  operator. The methods for producing such a component are discussed by many authors (Refs. 2, 3, 4). The basic circuit used in this investigation (Fig. 3) is given by P. R. Bell in Vol. 19 of the MIT Radiation Series (Ref. 4). It is a simple two-stage RC coupled amplifier with a positive feedback from the output of the second tube to the input grid of the first tube, and a negative feedback loop from the output of tube two to the cathode of tube one.

The reason for selecting the particular circuit used over others is that it appeared to be best suited to the desired frequency range.

Only the shunt negative capacitive reactance amplifier will be discussed here. A much more complete study of negative impedance production by the means of feedback amplifiers is given in Ginzton's article (Ref. 2).

For the sake of a simple explanation, imagine a two stage amplifier having zero phase shift, and a single positive feedback loop through the reactance  $X_N$ , as in Fig. 1. When a voltage  $e_1$  is applied to the input, the source supplies



BLOCK DIAGRAM OF NEGATIVE CAPACITY ELEMENT

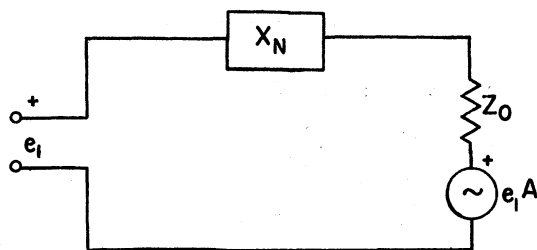
FIG. 1



a current,  $i_1$ . This current has the form

$$i_1 = e_1/Z_1 \quad (1)$$

where  $Z_1$  is the input impedance with feedback, and the input impedance without feedback is considered infinite (see Appendix A). The equivalent circuit is shown in Fig. 2.



THEVENIN EQUIVALENT OF BLOCK DIAGRAM  
OF NEGATIVE CAPACITY AMPLIFIER

FIG. 2

Thevenin's theorem gives the relation

$$e_1 = i_1(X_n + Z_o) + e_1A \quad (2)$$

where  $Z_o$  is the amplifier output impedance and  $A$  is the amplifier gain without feedback. Then by combining (1) and (2) we have

$$Z_1 = \frac{e_1}{i_1} = \frac{X_n + Z_o}{1-A} \quad (3)$$

In this expression it can be seen that  $Z_1$  is positive if  $A < 1$ ; increasing  $A$  causes  $Z_1$  to approach infinity, become negative, and have the value  $-(X_n + Z_o)$  where  $A = 2$ .

If an ideal amplifier could be produced, there is no reason why a simple two stage amplifier would not be good enough to produce a stable negative capacity over all frequencies, provided the negative resistance due to  $Z_o$  were

balanced out by a positive resistance connected to the input. But because an ideal amplifier does not exist, to improve the actual amplifier characteristics (i.e., stability and bandwidth), negative feedback is added to the basic amplifier as in Fig. 3. If the cathode resistors are considered unbypassed, degeneration due to this is included in the gain  $A$ . In addition, a feedback loop having a feedback fraction,  $\beta$ , is added from the output to the cathode of the first tube. This gives a new effective gain of the amplifier  $\mathcal{A}$  and substituting  $\mathcal{A}$  for  $A$  in equation (1), the input impedance becomes

$$Z_i = \frac{X_n + Z_o}{1 - \mathcal{A}} \quad (4)$$

where  $\mathcal{A} = \frac{A}{1 - A\beta}$

In an ideal amplifier  $Z_o$ ,  $A$ , and  $\mathcal{A}$  are real quantities and frequency insensitive. In an actual amplifier all of these quantities are complex, and frequency dependent. In addition, a small compensating capacity  $C_k$ , is introduced (see Fig. 3). These factors lead to a very involved expression for  $Z_i$  (see Appendix B).

The compensating capacitor  $C_k$  is introduced to extend the frequency response of the amplifier. It begins to reduce the cathode degeneration of the first stage at frequencies where the gain begins to fall off because of shunt capacitances. By a suitable adjustment, the upper frequency response of the amplifier may be increased with only slight variation in overall response.

Criteria established for the negative capacity element were: (1) wide bandwidth (as it was to operate over a wide frequency range), (2) capability of handling high input voltages (because of the voltages it may be subjected to in the oscillator tank circuit), (3) good stability, and (4) moderate plate power requirements. Tubes chosen to satisfy (4) may not satisfy (1) and (2) since these criteria are mutually exclusive.

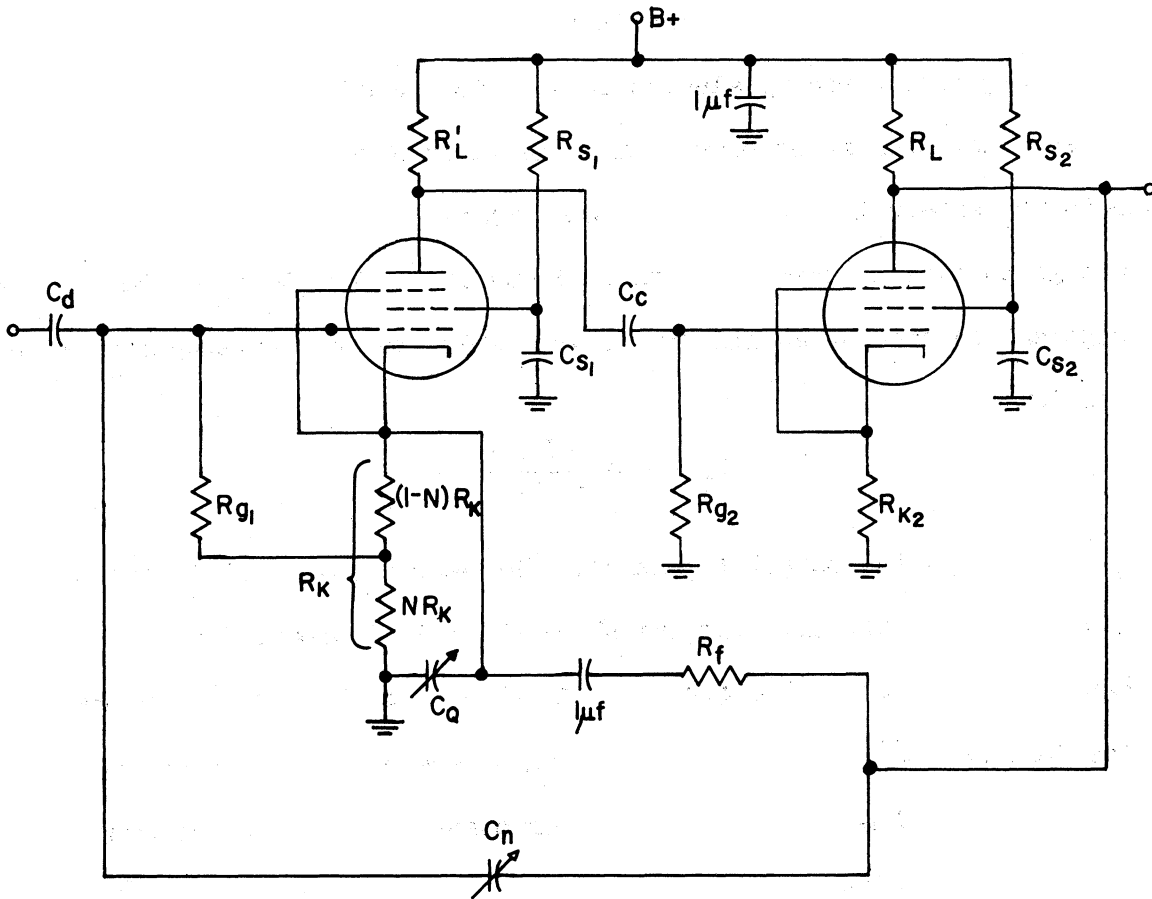


FIG. 3

CIRCUIT DIAGRAM OF THE NEGATIVE CAPACITY  
ELEMENT

If a parallel resonant circuit is placed at the input, oscillation takes place if the negative capacity element is able to overcome the external circuit power losses. This condition occurs when the input shunt conductance is negative and exceeds the external circuit shunt conductance in absolute magnitude. Two components go to make up this negative conductance. Since  $\mathcal{G} > 2$ , the first negative component is present at all times, and is due to the resistance term,  $R_0$ , in the expression

$$Z_i = \frac{X_n + X_0 + R_0}{1 - \mathcal{G}} \quad (5)$$

where  $R_0 + jX_0 = Z_0$ , the output impedance. The second component is introduced as the frequency becomes higher. Lagging phase shift is introduced due to tube and stray shunt capacitances in the circuit. At these frequencies  $\mathcal{G}$  becomes complex, taking the form  $\mathcal{G} = \mathcal{G}_r - j\mathcal{G}_i$ . At the point where  $j\mathcal{G}_i$  becomes appreciable,  $X_n$  and  $X_0$  render a second negative resistive component. The resistive component of  $Z_i$  is given in general by

$$R_i = \frac{(1 - \mathcal{G}_r)R_0 - \mathcal{G}_i(|X_n + X_0|)}{(1 - \mathcal{G}_r)^2 + \mathcal{G}_i^2} \quad (6)$$

Thus it is possible for the circuit to operate without oscillating at mid-band frequencies, while at higher frequencies the negative resistance  $R_i$  becomes large enough to cause oscillation.

Overloading the input voltage will also cause the circuit to oscillate. The overload voltage is determined by the plate characteristics at a given grid bias, and the amount of negative feedback in the circuit. Negative feedback will allow the input voltage to be increased by a factor of  $\frac{1}{(1-A\beta)}$  over overload voltage without negative feedback, within the normal operating frequency range.

If this circuit happens to be left ungrounded or open, it behaves as an asymmetric multivibrator operating at about 1000 cps. This is to be expected because the two tubes are capacitively inter-coupled.

### 3. EXPERIMENTAL RESULTS

#### 3.1 Actual Circuits

The circuit as given in Fig. 3 was built up using 6CL6 tubes. The transconductance is high ( $\cong 11,000 \mu\text{mho}$ ) in this type of tube. The values used in the circuit with this tube are given in Table I.

Other types of tubes can be used in the circuit, provided the inter-electrode capacities are low; such tubes are the 6AH6, 6AG5 or their octal equivalents. The circuit was built up using 6AG5's. The 6AG5 has the lowest  $g_m$  ( $\cong 5000 \mu\text{mho}$ ) of the three tubes considered. The components used in the 6AG5 circuit are also given in Table I. The results derived using this type of tube were very similar to those found using 6CL6 tubes with two expected differences. First, the circuit does not operate to quite as high a frequency (maximum of 2.5 mc as compared to somewhat over 3 mc for the 6CL6's). Second, the circuit is incapable of handling as high an input signal, primarily because of the lower bias on the 6AG5's. The type 6AH6 tube would probably give a circuit performance intermediate to that given by the 6AG5 and 6CL6 tube. The only advantage in using 6AG5 tubes was that the circuit required only 18 ma total plate current as compared to 70 ma with 6CL6's.

#### 3.2 Explanation of Graphs

Figures 4, 5, and 6 are plotted from data taken from the 6CL6 circuit. A Q-meter (Boonton 160A) was resonated at a given frequency with its internal capacitance. The Q was recorded. The negative capacity was placed in the circuit in parallel with the internal capacitance. The Q meter was re-resonated at the same frequency, and again the Q was recorded.

There are now three cases to consider. Either the Q is (1) higher with

TABLE I

Component Values Used in the Basic Circuit of Fig. 3

<u>Element</u>	<u>6CL6 Circuit</u>	<u>6AG5 Circuit</u>
$C_c$	.002 $\mu f$	.003 $\mu f$
$C_d$	.01 $\mu f$	.01 $\mu f$
$C_{s1}$	.5 $\mu f$	.5 $\mu f$
$C_{s2}$	.5 $\mu f$	.5 $\mu f$
$(1 - N)(R_k)$	100.	180.
$(N)(R_k)$	400.	680.
$R_{k2}$	100.	180.
$R_f$	1000.	3300.
$R_L$	1600.	10k
$R'_L$	1600.	10k
$R_{g1}$	1 meg	1 meg
$R_{g2}$	1 meg	1 meg
$R_{s1}$	22k	82k
$R_{s2}$	22k	82k
$g_m$	11 $\mu mho$	5 $\mu mho$
$C_n$	10-150 $\mu\mu f$ mica trimmer	10-150 $\mu\mu f$ mica trimmer
$C_k$	10-150 $\mu\mu f$ mica trimmer	10-150 $\mu\mu f$ mica trimmer
$C_o''$	Capacitance between the plate of tube 2 and ground	
$C_o'$	Capacitance between the plate of tube 1 and ground	

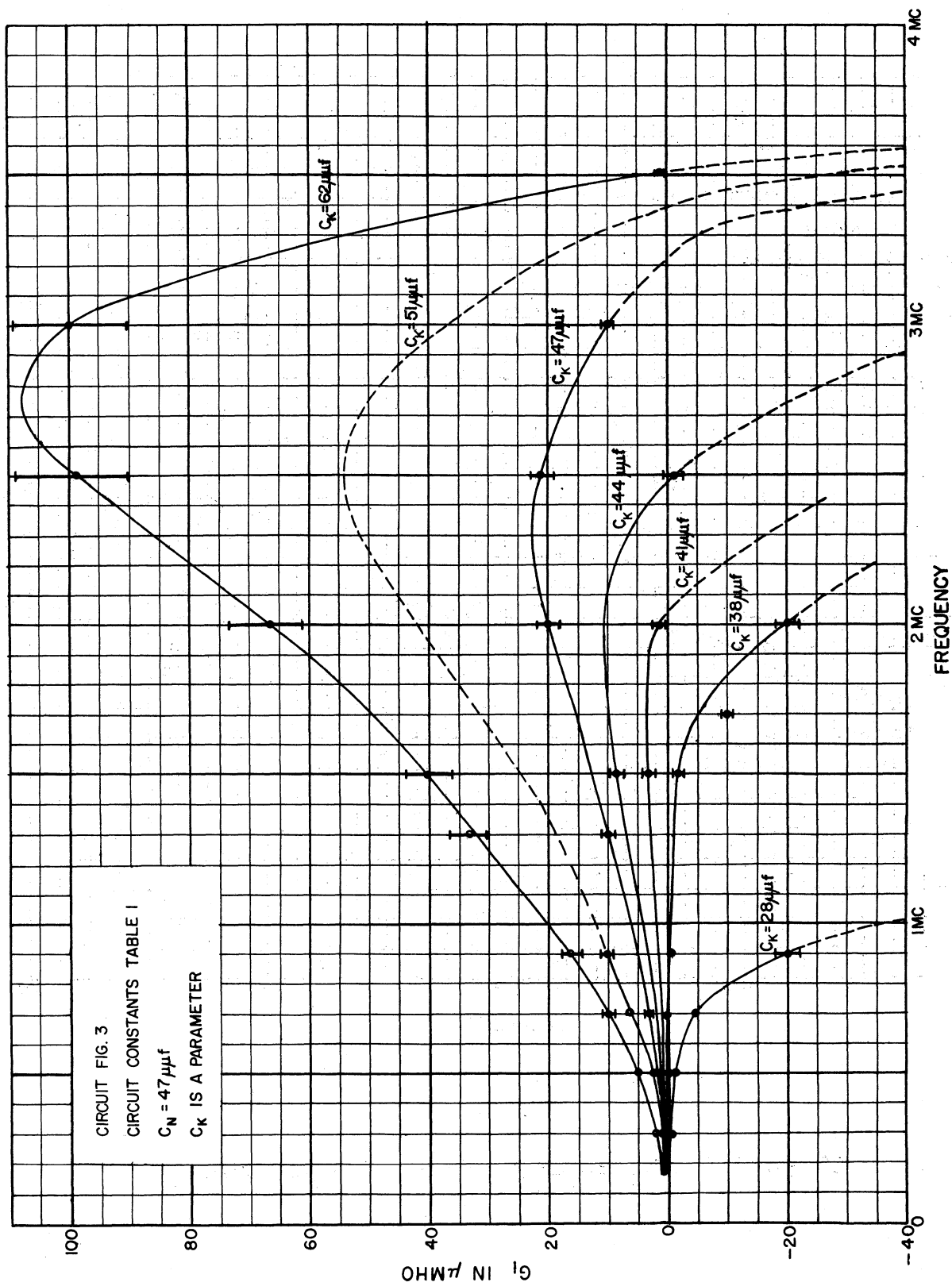


FIG. 4  
 GRAPH OF  $G_j$  VS. FREQUENCY WITH  $C_k$  AS A PARAMETER

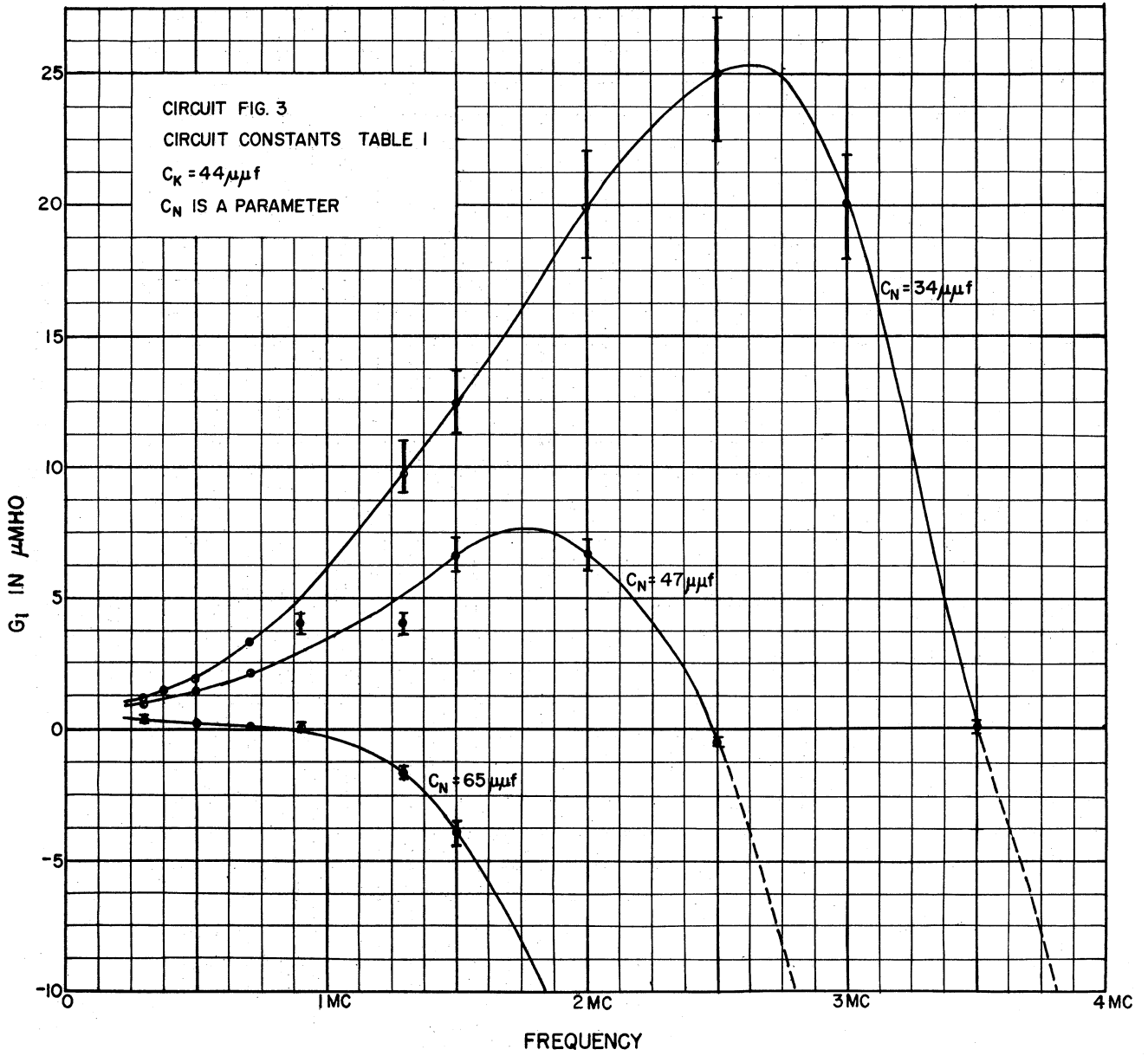


FIG. 5

GRAPH OF  $G_1$  VS. FREQUENCY WITH  $C_N$  AS A PARAMETER



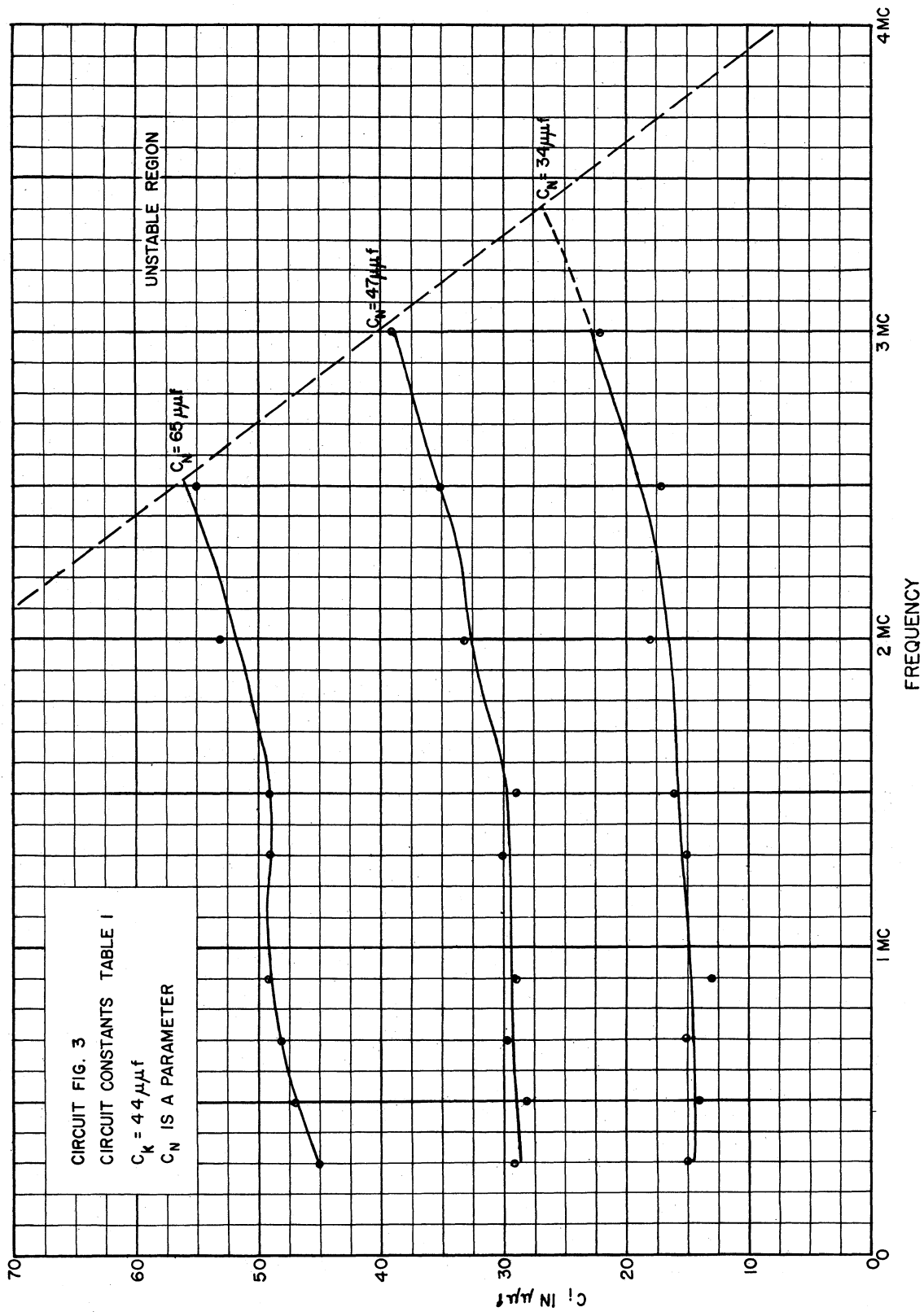


FIG. 6  
 GRAPH OF  $C_1$  VS. FREQUENCY WITH  $C_N$  AS A PARAMETER

the negative capacity, (2) the same, or (3) it is lower.

In case one, power is being supplied by the negative capacity to the Q-meter. The amount of negative conductance was determined by placing suitable resistance in shunt with negative capacity so that the value of  $Q$  for the Q-meter circuit was the same with and without the negative capacity. In case two, the negative capacity neither supplies, nor absorbs power. This means the input conductance is zero. In case three, power from the Q-meter is being supplied to the negative capacity. To determine this positive conductance, a resistor is shunted across the Q-meter without the negative capacity in the circuit. The above procedure was repeated for different frequencies from .3 mc to the point where, depending upon the value of  $C_n$  and  $C_k$ , oscillation could not be stopped with the introduction of a reasonable amount of positive conductance ( $\cong 100 \mu\text{mho}$ ).

In Figs. 4 and 5 the data points were obtained from the nominal values of the shunt resistors used. The range of possible error, indicated by the vertical bars, was obtained from the resistor tolerance.

The dashed lines on the graphs are estimates of the behavior of the conductance when no data were taken.

Figure 6 shows a plot of negative capacitance as a function of frequency. The negative capacity oscillates in the region to the right of the diagonal dashed line.

In Figures 4 and 5 it is noticed that the conductance starts out positive and quite low, increases to a maximum, and then goes negative very steeply as the frequency increases. With increasing  $C_k$ , or decreasing  $C_n$ , the positive conductance maximum increases in magnitude and occurs at higher frequencies. This is to be expected from the analytical derivation of  $Y_1$  (see Appendix B). The shape of the  $C_1$  vs. frequency curves is also predicted by this derivation.

### 3.3 Summary of Results

Satisfactory operation was obtained only when the circuit was not overloaded. Although extensive data were not taken, the overload voltage appeared to decrease as the frequency was increased. It also decreased as  $C_n$  was increased.

Using the 6AG5 circuit, the overload voltage at 2 mc had decreased to 1.9 volts rms for  $C_n = 41\mu\text{f}$ , but to only 2.7 volts rms for  $C_n = 10\mu\text{f}$ . This circuit was used in conjunction with a one tube oscillator (Fig. 7) to investigate the possible improvement in tuning range. So long as the oscillator tank voltage was below the overload point, an improvement in tuning range was obtained up to about 2.5 mc. Above this frequency, the negative capacity began to take control of the frequency of the tank circuit, raising it to a somewhat higher frequency ( $\approx 4$  mc).

Near a region where the negative capacity controls the oscillation, increasing  $C_n$  first increases the frequency of oscillation (from  $\approx 2$  to  $\approx 4$  mc and upward) then causes it to oscillate at a much lower frequency ( $\approx .9$  mc). This indicates that as  $C_n$  is increased the negative capacity first increases very sharply (2 to 4 mc) and then continues to increase more slowly. With a further increase in  $C_n$ , the input capacity becomes positive.

Limitations are imposed on the amount of negative capacity that can be added to the circuit. From Fig. 5 it is seen that increasing  $C_i$  negatively (e.g.,  $C_n$ ) lowers the frequency where negative conductance appears. For this reason the amount of negative capacity added must be such that the total capacity is large enough to resonate at a frequency below the negative conductance region.

Examples of this are given in the following data:

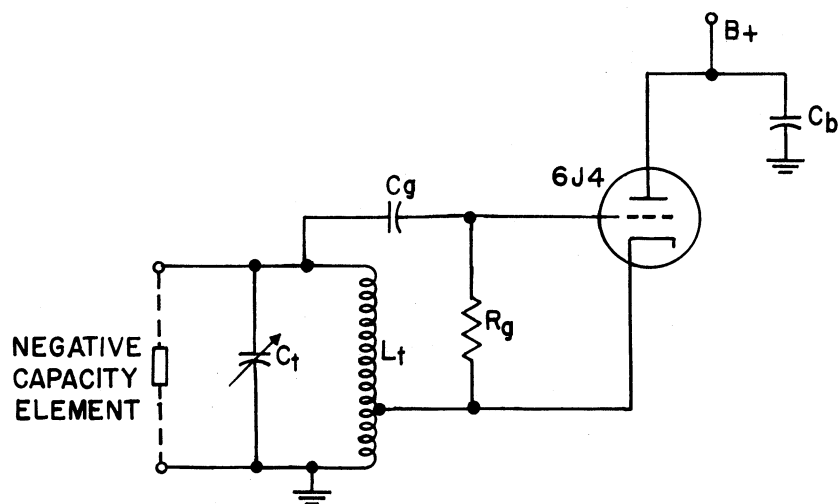


FIG. 7

OSCILLATOR CIRCUIT USED IN CONJUNCTION  
WITH THE NEGATIVE CAPACITY ELEMENT

$C_i$ $\mu\mu f$	$C_t$ $\mu\mu f$	Measured Upper Frequency Limit (Megacycles)
-20	44	1.8
-24	64	~1.5
-26	71	~1.4

where  $C_t$  is the tank capacitance, including strays.

When using  $C_i = -20\mu\mu f$  the tuning range can be extended from approximately 2:1 to 2.7:1 as given in the following data:

$C_i$ $\mu\mu f$	$C_t$ $\mu\mu f$	Measured Resonant Frequency (Megacycles)	Tuning Range
none	44	1.26	2:1
none	184	.63	
-20	44	1.8	2.7:1
-20	184	.67	

The upper frequency limit for satisfactory operation could be raised by employing (1) cathode peaking in the second tube, (2) lower plate loads, or (3) shunt plate peaking.

### 3.4 Application to Dielectric Tuned Receivers

An application of the negative capacity might be realized in a dielectric tuned receiver. Because the negative capacity's input voltage is limited it cannot be used in the local oscillator. But in the rf and mixer stages, the negative capacity could be used to advantage. Fig. 8 shows the tuning curves of a

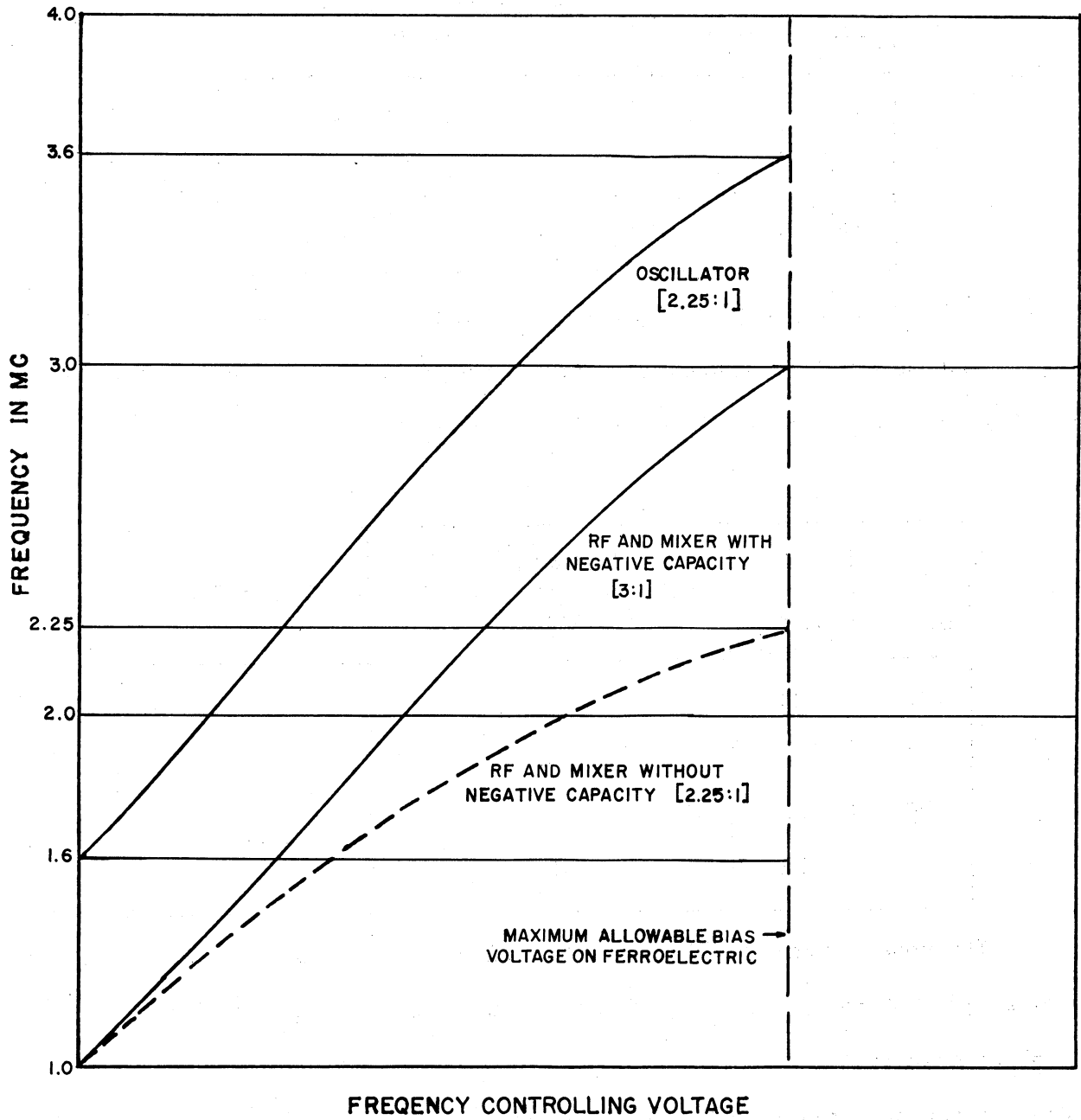


FIG. 8  
TUNING CURVES OF A DIELECTRIC TUNED RECEIVER

dielectric tuned receiver. The local oscillator is designed to give a 600 kc intermediate frequency. In this example, the tuning range without negative capacity for the oscillator, rf and mixer stages is 2.25:1 for the maximum allowable ferroelectric bias field. The desired frequency range of the receiver is from 1 to 3 mc. The local oscillator can cover this range with no difficulty because it tracks the mixer tuning unit at 0.6 mc above, therefore the maximum range of the oscillator (1.6 to 3.6 mc.) is only 2.25:1. The rf and mixer stages can cover only the range 1 to 2.25 mc, however. If a negative capacity of the proper value is added to these stages, they will now tune from 1 to 3 mc giving the required increase in tuning range of the entire receiver.

#### 4. CONCLUSION

The negative capacity amplifier was found to operate satisfactorily in a restricted frequency range below 3 mc. The upper frequency limit can be raised somewhat with suitable circuit modifications.

Because the negative capacity element is capable of handling very small input voltages it is limited to use in rf amplifiers and certain applications in rf oscillators where it is not subjected to more than 3 or 4 volts (rms) of alternating voltage.

APPENDIX AApproximation for  $Z_1$ 

$Z_1$ , the input impedance with feedback is (as shown in the Eq. 4) dependent upon the output impedance, the circuit gain and  $C_n$ .

However, if  $R$  is finite,  $Z_1$  takes the form

$$Z_1 = \frac{R(X_n + Z_o)}{(1 - \mathcal{G})(R + X_n + Z_o)} \quad (7)$$

where  $Z_o$  is the output impedance of the amplifier and  $R$ , the dynamic input resistance in the absence of feedback through  $X_n$ , has the form

$$R = R_g \left( \frac{1}{1 - \frac{\mathcal{G}}{A}} \right) N = \frac{AR_g}{A - N(A - \mathcal{G})} \quad (8)$$

where  $N$  is the fraction from ground of the cathode resistor at the point of the  $R_g$  connection, and  $R_g$ ,  $\mathcal{G}$ , and  $A$  are as previously defined.

In the circuit used,  $R = 5$  megohms and, therefore, at least two orders of magnitude larger than  $X_n$  or  $Z_o$ . Therefore, Eq. 7 may be closely approximated by

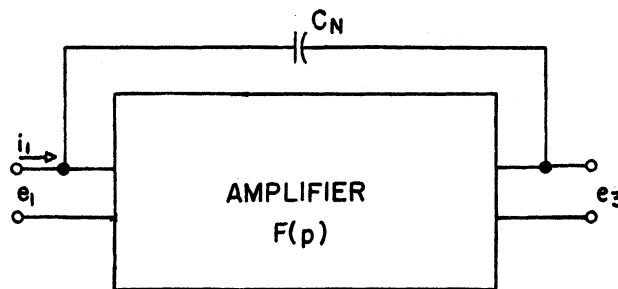
$$Z_1 = \frac{X_o + Z_o}{1 - \mathcal{G}} \quad (4)$$



APPENDIX B

In studying the input conductance as shown in Figs. 4 and 5 it is more convenient to look at the input admittance rather than input impedance. The input admittance is given by

$$Y_i = \frac{i_1}{e_1} = \left( \frac{e_3 - e_1}{e_1} \right) j\omega C_n \quad (\text{See Fig. 9}) \quad (9)$$



BLOCK DIAGRAM OF NEGATIVE CAPACITY AMPLIFIER

FIG. 9

$$Y_i = [F(p) - 1] pC_n \quad (10)$$

where  $p = j\omega$  and  $F(p) = \frac{e_3}{e_1}$  is a function of  $p$  to be found in the following sections.

The input admittance will be calculated on a somewhat simplified version (Fig. 9) of the circuit as given in Fig. 3. The tube transconductance,  $g_m$ , is modified by cathode degeneration to  $g_m$  given approximately by

$$g_m = \frac{g_m}{g_m R_k + 1} \quad (11)$$

where  $R_k$  is the cathode resistor, and  $g_m$  is the effective transconductance of the tube in question assuming that the screen current is a small percentage of the

total cathode current.

Replacing the loads and tubes of Fig. 10 by admittances and current generators we obtain Fig. 11, the equivalent current generator circuit.  $e_1$  is the input voltage to the first tube grid (no grid current is assumed to flow in either tube).  $e_2$  is the voltage across  $Y_2$ , which is the input to the second tube.

The second tube is replaced by a current generator  $I_2 = e_2 gm_2$ , and  $e_3$  is the output voltage.

$e_k$  is the voltage across  $Y_k$ , the cathode admittance.

The nodal equations at A, B, and K are as follows

$$e_1 gm_1 = G_p' (e_2 - e_k) + Y_2 e_2 \quad (12)$$

$$e_2 gm_2 = Y_3 e_3 + G_f (e_3 - e_k) \quad (13)$$

$$e_1 gm_1 = G_f (e_3 - e_k) + G_p' (e_2 - e_k) - Y_k (e_k) \quad (14)$$

solving for  $\frac{e_3}{e_1} = F(p) \frac{-gm_1 G_f Y_2 + gm_1 gm_2 (G_f + Y_k)}{G_f Y_3 (G_p' + Y_2) + Y_3 + G_f G_p' Y_2 + Y_k (Y_3 + G_f) (G_p' + Y_2) - gm_2 G_f G_p'}$  (15)

Substituting the components for the complex admittances  $Y_k, Y_3, Y_2$  and factoring powers of  $p$  we have

$$Y_1 = \left[ \frac{P+Qp}{R+Sp+Tp^2 + Up^3} - 1 \right] p C_n \quad (16)$$

where coefficients P, Q, R, S, T, and U are as follows:

$$P = gm_1 [gm_2 (G_f + G_k) - G_f G_L'] \quad (17)$$

$$Q = gm_1 [gm_2 C_k - G_f C_o'] \quad (18)$$

$$R = G_f G_3 G_2 + (G_3 + G_f) G_p' G_L' + G_k (G_3 + G_f) G_2 - gm_2 G_f G_p' \quad (19)$$

where  $G_2 = G_p' + G_L'$

and  $G_3 = G_p'' + G_L''$

$$S = G_f (G_3 C_o' + G_2 C_o'') + G_p' \{ C_o' (G_3 + G_f) + C_o'' G_1 \} + G_k (G_3 + G_f) C_o' + G_k G_2 C_o'' + (G_3 + G_f) G_2 C_k \quad (20)$$

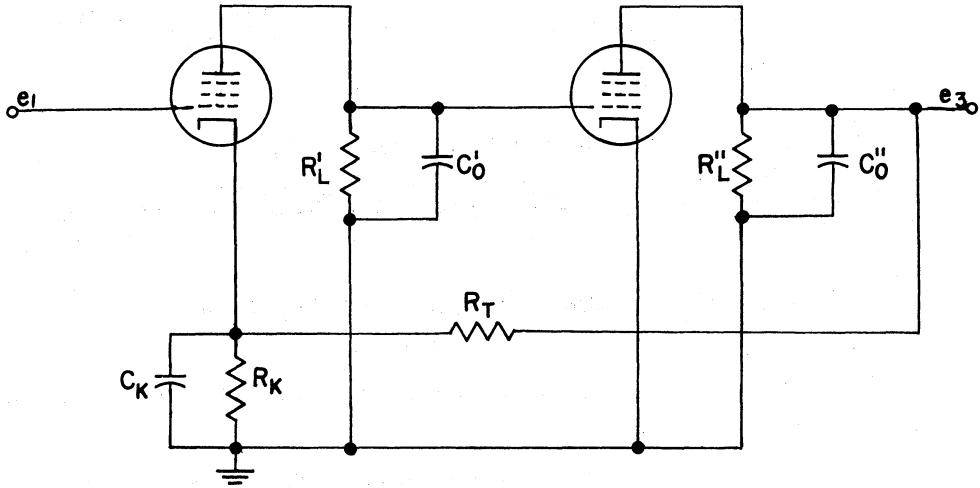


FIG. 10

SIMPLIFIED CIRCUIT OF NEGATIVE CAPACITY AMPLIFIER

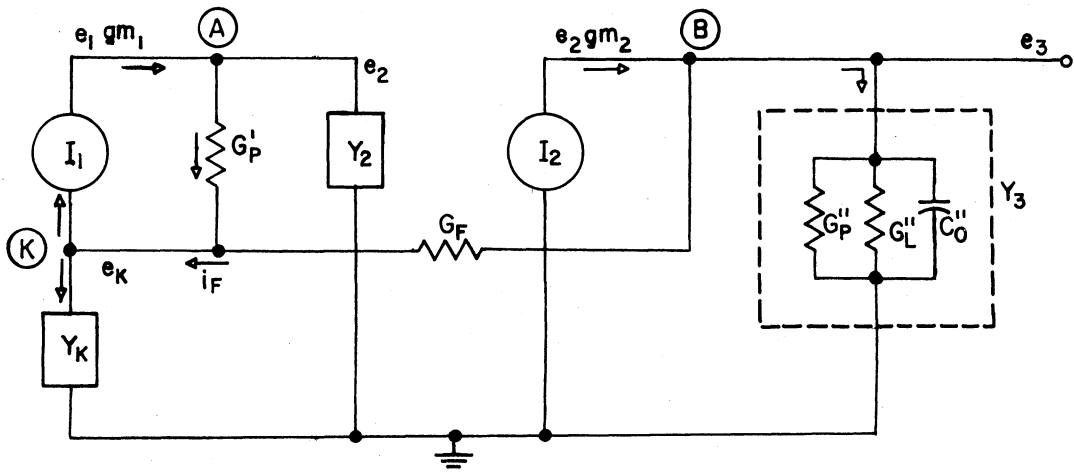


FIG. 11

EQUIVALENT CURRENT GENERATOR CIRCUIT OF FIGURE 8

$$T = C_o''C_o'(G_f+G_p') + G_kC_o''G_2 + C_kC_o'(G_3+G_f) + G_kC_o''C_o' \quad (21)$$

$$U = C_kC_o''C_o' \quad (22)$$

expanding  $F(p)$  in powers of  $p$  and substituting in Eq. 10

$$Y_1 = pC_n \left[ \frac{P}{R} - 1 + \frac{QR-PS}{R^2} p - \left\{ \frac{(QR-PS)S+PRT}{R^3} \right\} p^2 + \text{higher order terms in } p \right] \quad (23)$$

$\left(\frac{P}{R} - 1\right) pC_n$  is the negative capacity term

$\left[ \left(\frac{QR-PS}{R^2}\right) p \right] pC_n$  is a negative resistive term which depends upon  $\omega^2$ .

The coefficient of  $p^3$  is another capacitive term and that of  $p^4$  another resistive term, etc.

Plots of input conductance and capacitance based on Eq. 23 give curves similar to Figs. 4, 5 and 6.

REFERENCES

1. { Howard Diamond and L. W. Orr, "Interim Report on Ferroelectric Materials and Applications," EDG Tech. Rep. No. 31, July 1954.  
L. W. Orr, "Ferromagnetic and Ferroelectric Tuning," EDG Tech. Rep. No. 32, August 1954.
2. E. L. Ginzton, "Stabilized Negative Impedances Parts I and II," Electronics, July and August 1945.
3. Herbert J. Reich, "Theory and Application of Electron Tubes," McGraw-Hill, 1944, pp. 211-216.
4. Chance, Hughes, MacNickel, Sayre, Williams, "Waveforms," MIT Radiation Laboratory Series, Vol. 19, Appendix A (P. E. Bell), McGraw-Hill, 1948.

DISTRIBUTION LIST

1 copy            Director, Electronic Research Laboratory  
Stanford University  
Stanford, California  
Attn: Dean Fred Terman

1 copy            Chief, Electronic Warfare Department  
Army Electronic Proving Ground  
Fort Huachuca, Arizona

1 copy            Chief, Engineering and Technical Division  
Office of the Chief Signal Officer  
Department of the Army  
Washington 25, D. C.  
Attn: SIGJM

1 copy            Chief, Plans and Operations Division  
Office of the Chief Signal Officer  
Washington 25, D. C.  
Attn: SIGOP-5

1 copy            Countermeasures Laboratory  
Gilfillan Brothers, Inc.  
1815 Venice Blvd.  
Los Angeles 6, California

1 copy            Commanding Officer  
White Sands Signal Corps Agency  
White Sands Proving Ground  
Las Cruces, New Mexico  
Attn: SIGWS-CM

1 copy            Commanding Officer  
Signal Corps Electronics Research Unit  
9560th TSU  
Mountain View, California

75 copies        Transportation Officer, SCEL  
Evans Signal Laboratory  
Building No. 42, Belmar, New Jersey

FOR - SCEL Accountable Officer  
Inspect at Destination  
File No. 22824-PH-54-91(1701)

1 copy            H. W. Welch, Jr.  
                  Engineering Research Institute  
                  University of Michigan  
                  Ann Arbor, Michigan

1 copy            Document Room  
                  Willow Run Research Center  
                  University of Michigan  
                  Willow Run, Michigan

1 copy            Engineering Research Institute Project File  
                  University of Michigan  
                  Ann Arbor, Michigan

11 copies        Electronic Defense Group Project File  
                  University of Michigan  
                  Ann Arbor, Michigan

UNIVERSITY OF MICHIGAN



3 9015 02523 0197